Brownian Dynamics Simulation of Knot Diffusion along a Stretched DNA Molecule

Alexander Vologodskii
Department of Chemistry, New York University, New York, New York

ABSTRACT   Manipulation of individual DNA molecules by optical tweezers has made it possible to tie these molecules into knots. After stretching the DNA molecules the knots become highly localized. In their recent study, Quake and co-authors investigated diffusion of such knots along stretched DNA molecules. We used these data to test the accuracy of a Brownian dynamics simulation of DNA bending motion. We simulated stretched DNA molecules with knots 3_1, 4_1, and 7_1, and determined their diffusion coefficients. Comparison of the simulated and experimental results shows that Brownian dynamics simulation is capable of predicting the rates of large-scale DNA rearrangements within a factor of 2.

INTRODUCTION

Brownian dynamics (BD) is an efficient computational method allowing the simulation of large-scale conformational dynamics of macromolecules (1). Over the last 20 years the method has been applied to study various dynamic properties of linear and circular DNA molecules (2–10). It has been shown that the method predicts equilibrium conformational properties of DNA (11) and its translational and rotational diffusion coefficients (2,5,11). The diffusion coefficients, however, are not sensitive to the rate of the internal dynamics of DNA bending, and can be equally well calculated by averaging over the equilibrium conformational ensemble (12,13). Until recently, there were very limited quantitative experimental data on the dynamics of DNA bending (14), and therefore it was difficult to test how well the method describes this kind of motion. The situation changed when Quake and co-authors performed a study of knot diffusion along stretched DNA (15). To tie a knot on a single DNA molecule one has to manipulate its contour. Arai et al. (16) were the first authors we know of to solve this problem by using optical tweezers and placing DNA into a medium with high viscosity. A flow of the medium facilitated straightening DNA contour and tying knots on long DNA molecules, which accept random coil conformation under normal conditions (15). Stretching the knotted molecules resulted in highly localized knots (Fig. 1). Monitoring the position of the knots versus time, the researchers measured the diffusion coefficients of different knots (15). Clearly, knot diffusion is directly related to the bending dynamics of DNA molecules. Thus, the study by Bao et al. provided experimental data that can be used to test the accuracy of BD simulations of DNA internal motion. Here we simulate the diffusion of knots along a stretched DNA

molecule, calculate the knot diffusion coefficients, and compare the results with the experimental data. Such a comparison is a goal of the current study.

DNA MODEL AND METHODS OF CALCULATIONS

DNA model

Our DNA model is based on the discrete wormlike chain and is similar to one developed by Allison et al. (2,17) and by Langowski and co-workers (5,8). A careful adaptation, parameterization, and testing of the model for linear DNA was described earlier (11).

A DNA molecule composed of n Kuhn statistical lengths is modeled as a chain of kn straight elastic segments of equilibrium length l_0. The chain energy consists of the following four terms.

1. The stretching energy is computed as

$$E_s = \frac{h}{2} \sum_{i=1}^{nk} (l_i - l_0)^2, \tag{1}$$

where l_i is the actual length of segment i, and h is the stretching rigidity constant. The energy E_s should be considered as a computational device rather than an attempt to account for the actual stretching elasticity of the double helix. Smaller values of h allow larger time steps in the BD simulations, but also imply larger departures from l_0 (11). We choose $h = 100\, k_B T/l_0^2$, where $k_B T$ is the Boltzmann temperature factor, so that the variance of l_i is close to $l_0^2/100$ for this value of h.

2. The bending energy, E_b, is specified by angular displacements θ_i of each segment $(i + 1)$ relative to segment i:

$$E_b = \frac{g}{2} \sum_{i=1}^{kn-1} \theta_i^2. \tag{2}$$

The bending rigidity constant g is defined such that a Kuhn statistical length corresponds to k rigid segments (18). It was shown previously that the majority of DNA equilibrium properties do not change, within the accuracy of the simulations, if $k \geq 10$ (19). The value $k = 10$ used here corresponds to $g = 4.81\, k_B T$ and $l_0 = 10$ nm when using 100 nm for the Kuhn length (20).

3. The energy of electrostatic intersegment interaction, E_e, is specified by the Debye-Hückel potential as a sum over all pairs of point charges located on the chain segments. The number of point charges placed on each segment, λ, is chosen to approximate well continuous charges with the same linear density. The value of λ should be increased as the

FIGURE 1 Diffusion of a tight knot along a stretched DNA molecule. The diagram illustrates the experimental design of the system (15). DNA is attached to the beads, which are manipulated by optical tweezers. The stretching force, F, is applied to the beads. The simulated conformation of a DNA molecule 3000 bp in length was used for the illustration. DNA molecules 16 times longer were used in the experiments.

Debye length, $1/\kappa$, decreases. The experimental data by Bao et al. (15), modeled here, were obtained for $[Na^+] = 0.01$ M. For these conditions we have found that $\lambda = 2$ is sufficient (11). The value of λ used in the current study was equal to 1 or 2, and the simulation results were indistinguishable. The energy E_e is specified as

$$E_e = \frac{\nu^2 l_o^2}{\lambda^2 D} \sum_{i,j}^{N} \frac{\exp(-\kappa r_{ij})}{r_{ij}}, \qquad (3)$$

where ν is the effective linear charge density of the double helix, D is the dielectric constant of water, $N = kn\lambda$ is the total number of point charges, and r_{ij} is the distance between point charges i and j. The value of ν is equal to 2.43 e/nm for $[Na^+] = 0.01$ M (21). This value of ν corresponds to the solution of the Poisson-Boltzmann equation for DNA modeled as a charged cylinder. It was found by Stigter (21) that this solution can be approximated well by the Debye-Hückel potential for the charged line. This approximation requires only a suitable definition of ν to match the potential-distance curve in the overlap region far from the cylindrical surface.

The electrostatic interaction contributes both to the bending rigidity of the double helix and to the volume interaction between chain segments separated along the chain contour. Since the first effect is already taken into account for the experimentally measured value of the bending rigidity constant, the interaction between charges located at adjacent segments was not included in Eq. 3.

4. The energy of the short-range repulsion between DNA segments, E_v, is added to the energy function to prevent passing one segment through another, since the electrostatic repulsion, specified above, does not exclude this. E_v can be introduced as

$$E_v = -\sum_{i,j}^{N} \mu r_{ij} \text{ if } r_{ij} < 2 \text{ nm}$$

$$E_v = 0 \text{ if } r_{ij} > 2 \text{ nm}, \qquad (4)$$

where summation is performed over the same pairs of points as in Eq. 3. It was found that for $\mu = 35$ pN the frequency of segment passing events is $< 10^{-7}$ per simulation step (10). Since the simulation runs of up to 10^8 steps were used in this study, we determined the chain topology after each 10^5 steps and recorded the current conformation if the topology was unchanged. To determine topology of a particular chain conformation we calculated the Alexander polynomial for this conformation (see below). If the topology was changed since the last recording, we returned to the recorded conformation and repeated the simulation from the time of recording with a different seed number.

It should be noted that the shape of this additional potential, specified by Eq. 4, has an absolutely negligible effect on the dynamic properties of the model chain. It was added only to reduce the probability of passing one segment through another during the simulation. We chose the potential to be as smooth as possible, so it would not require decreasing the integration time step (10). There is very strong electrostatic repulsion between the chain segments (Eq. 3), so it is extremely rare that the distance between two

segments becomes smaller than the geometrical diameter of the double helix and the additional potential acts.

To account for hydrodynamic interactions of the DNA with solvent we positioned beads of radius a at each vertex of the chain. These beads are only used to define the hydrodynamic interaction and thus do not affect equilibrium properties of the model chain. We used the Rotne-Prager diffusion tensor to specify the hydrodynamic interaction (22). The value of a was equal to 2.24 nm. This value was chosen to provide the experimentally measured values of the translational diffusion (sedimentation) coefficients of circular DNA (13,23,24).

Brownian dynamics simulations

We use the second-order BD algorithm (25) with modifications to improve efficiency (7,11), involving less frequent updating of the diffusion tensor than the systematic forces (e.g., every 10 time steps). This does not compromise the numerical accuracy, whereas the CPU time is reduced on average by a factor of four (7,8,11).

Initial conformation of the chain with a knot located near the chain middle (Fig. 1) was equilibrated by a preliminary simulation run. Chain topology was monitored by calculating the Alexander polynomial $\Delta(t)$ for $t = -1$ and $t = -2$ (26). Although topological invariants for knots are defined for closed contours only, it is easy to extend the polynomial calculation for stretched linear chains considered here.

The time step Δt of 500 ps was used throughout these computations; ~ 2 h of computing are required on Power Mac G5, 2.5 GHz processor to simulate 1 ms of 3000 bp DNA. The simulation time grows rapidly, however, as the chain length increases (11). Therefore, to perform reliable estimation of the knot diffusion coefficients we used the following technique. The simulations were performed for chains of 80–120 segments (2400–3600 bp), but each time a knot approached one end of the chain, we cut a subchain at the other end of the molecule and attached it to the short end. Since there is a limited correlation between the motion of different parts of the chain, this procedure did not affect the diffusion process. Thus, we virtually simulated the diffusion along the infinite chain, keeping the simulation speed high. The total length of the simulated trajectories was ~ 100 ms for each of three knots studied here.

To calculate a knot position, S_k, along the chain we first determined all segments of the chain that intersect other segments when projected on a plane parallel to the direction of the force. Since the chain was strongly extended by the force, only segments of the knot intersect one another. The value of S_k was calculated as

$$S_k = \frac{1}{2M} \sum_{i}^{M} (n_i^1 + n_i^2), \qquad (5)$$

where the sum is taken over all intersections, M is the number of intersections, and n_i^1 and n_i^2 are the segments participating in the intersection i.

RESULTS AND DISCUSSION

We studied, by BD simulation, the diffusion of knots 3_1, 4_1, and 7_1 along a stretched DNA molecule (Fig. 2). The force, applied to both ends of the model chain, was equal to 0.5 pN over all the simulations performed in this work, which is in the middle of the force range used by Bao et al. (15). First, we compared computed lengths of the knots, L_k, with the corresponding values determined experimentally. We calculated L_k as

$$L_k = \langle x \rangle_0 - \langle x \rangle_k, \qquad (6)$$

where $\langle x \rangle_k$ is the average extension of the chain with a particular knot and $\langle x \rangle_0$ is the extension of the unknotted
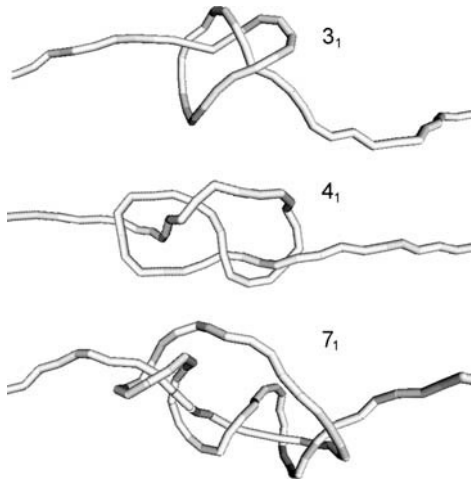
FIGURE 2 Knots 3_1, 4_1, and 7_1. Typical simulated conformations of the knots are shown.

FIGURE 3 Determination of the knot diffusion coefficients, D_k. Equation 7 was used to calculate the values of D_k by averaging the displacement over the time interval Δt along the entire simulation runs. The calculated values of D_k are plotted for knots 3_1, 4_1, and 7_1 as a function of Δt.

chain of the same contour length. The results of this determination are shown in Table 1 together with the experimental values obtained by Bao et al. (15). The simulated values of L_k are 25–30% shorter than the experimental ones. This difference exceeds statistical experimental error by a factor of ~2 (15). It is not clear, however, if the discrepancy is meaningful or results from some systematic experimental error.

To estimate the knot diffusion coefficient, D_k, we recorded, each 50 μs, the position of the knot along the contour of the model chain over the long simulation runs. At the end, all trajectories for a particular knot were combined; their total lengths are shown in Table 1. The value of D_k was calculated by applying the equation

$$\langle \Delta x^2 \rangle = 2D_k(\Delta t), \qquad (7)$$

where Δx is the knot displacement over the time interval Δt. For a particular value of Δt, the sliding average of Δx^2 was calculated over all recorded positions of the knot. Fig. 3 shows that different values of Δt used in the analysis give close estimations for D_k. One can see from the figure that the simulated values of D_k decrease with growing complexity of the knots, as was observed by Bao et al. (15).

The values of D_k found by this method turned out to be 1.3 to 1.9 times lower than the corresponding values obtained experimentally (Table 1). The data obtained by Bao et al.
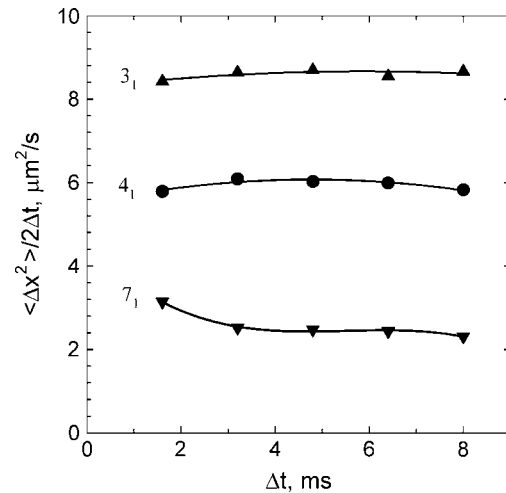
(15) suggest one possible explanation for this discrepancy. Bao et al. found that the measured values of $\langle \Delta x^2 \rangle$ as a function of Δt slightly deviate from Eq. 7. The data are better described by a nonlinear dependence of $\langle \Delta x^2 \rangle$ vs. Δt,

$$\langle \Delta x^2 \rangle \propto (\Delta t)^{\alpha}, \qquad (8)$$

with $\alpha = 1.06 \pm 0.02$. Naturally, Bao et al. assumed that this result is in agreement with Eq. 7, which must be held for a one-dimensional diffusion process. To calculate D_k they plotted $\langle \Delta x^2 \rangle$ vs. Δt on linear axes and fitted by a straight line, leaving the offset term free to compensate for short-time artifacts from both observation and analysis (15). Slopes obtained from these fits were considered to be equal to $2D_k$. This procedure of estimating D_k and the deviation of α from 1 can explain, however, the large part of the difference between the simulated and experimental results, since the values of Δt used in our analysis are three orders of magnitude smaller than the values used by Bao et al. (15). Thus, the accuracy of the BD simulation of DNA bending could be better than the current comparison shows.

We consider, however, that the ability of the BD simulations to predict rates of different rearrangements in large DNA molecules within a factor of 2 is really remarkable if we take into account that there were no adjustable

TABLE 1 Comparison of the simulated and experimental knot lengths and diffusion coefficients

Knot type	Total length of simulated trajectories (ms)	Knot length, simulated (μm)	Knot length, experimental (μm)	Computed diffusion coefficient (μm^2/s)	Measured diffusion coefficient (μm^2/s)
3_1	222	0.20 ± 0.01	0.25 ± 0.02	8.6 ± 1	12.5 ± 0.5
4_1	237	0.26 ± 0.01	0.38 ± 0.03	6.0 ± 1	7.9 ± 0.3
7_1	165	0.46 ± 0.01	0.56 ± 0.03	2.5 ± 0.3	4.8 ± 0.2

The experimentally measured values were taken from Fig. 2a of Bao et al. (15) and adjusted to the water viscosity according to a personal communication with S. R. Quake (Stanford University, 2005).

parameters in the simulations. Clearly, the BD simulation of DNA large-scale dynamics can be used as a valuable tool to address different biologically related problems.

REFERENCES

1. Ermak, D. L., and J. A. McCammon. 1978. Brownian dynamics with hydrodynamic interactions. *J. Chem. Phys.* 69:1352–1360.

2. Allison, S. A. 1986. Brownian dynamics simulation of wormlike chains. Fluorescence depolarization and depolarized light scattering. *Macromolecules.* 19:118–124.

3. Allison, S., R. Austin, and M. Hogan. 1989. Bending and twisting dynamics of short DNAs. Analysis of the triplet anisotropy decay of a 209 base pair fragment by Brownian simulation. *J. Chem. Phys.* 90:3843–3854.

4. Allison, S. A., S. S. Sorlie, and R. Pecora. 1990. Brownian dynamics simulations of wormlike chains: dynamic light scattering from a 2311 base pair DNA fragment. *Macromolecules.* 23:1110–1118.

5. Chirico, G., and J. Langowski. 1992. Calculating hydrodynamic properties of DNA through a second-order Brownian dynamics algorithm. *Macromolecules.* 25:769–775.

6. Chirico, G., and J. Langowski. 1996. Brownian dynamics simulations of supercoiled DNA with bent sequences. *Biophys. J.* 71:955–971.

7. Jian, H., T. Schlick, and A. Vologodskii. 1998. Internal motion of supercoiled DNA: Brownian dynamics simulations of site juxtaposition. *J. Mol. Biol.* 284:287–296.

8. Klenin, K., H. Merlitz, and J. Langowski. 1998. A Brownian dynamics program for the simulation of linear and circular DNA and other wormlike chain polyelectrolytes. *Biophys. J.* 74:780–788.

9. Podtelezhnikov, A. A., and A. V. Vologodskii. 2000. Dynamics of small loops in DNA molecules. *Macromolecules.* 33:2767–2771.

10. Huang, J., T. Schlick, and T. Vologodskii. 2001. Dynamics of site juxtaposition in supercoiled DNA. *Proc. Natl. Acad. Sci. USA.* 98: 968–973.

11. Jian, H., A. Vologodskii, and T. Schlick. 1997. Combined wormlike-chain and bead model for dynamic simulations of long linear DNA. *J. Comput. Phys.* 73:123–132.

12. Hagerman, P. J., and B. H. Zimm. 1981. Monte Carlo approach to the analysis of the rotational diffusion of wormlike chains. *Biopolymers.* 20:1481–1502.

13. Rybenkov, V. V., A. V. Vologoskii, and N. R. Cozzarelli. 1997. The effect of ionic conditions on the conformations of supercoiled DNA. I. Sedimentation analysis. *J. Mol. Biol.* 267:299–311.

14. Heath, P. J., J. A. Gebe, S. A. Allison, and J. M. Schurr. 1996. Comparison of analytical theory with Brownian dynamics simulations for small linear and circular DNAs. *Macromolecules.* 29:3583–3596.

15. Bao, X. R., H. J. Lee, and S. R. Quake. 2003. Behaviour of complex knots in single DNA molecules. *Phys. Rev. Lett.* 91:265506.

16. Arai, Y., R. Yasuda, K. Akashi, Y. Harada, H. Miyata, K. J. Kinosita, and H. Itoh. 1999. Tying a molecular knot with optical tweezers. *Nature.* 399:446–448.

17. Allison, S. A., and J. A. McCammon. 1984. Multistep Brownian dynamics: application to short wormlike chains. *Biopolymers.* 23: 363–375.

18. Frank-Kamenetskii, M. D., A. V. Lukashin, V. V. Anshelevich, and A. V. Vologodskii. 1985. Torsional and bending rigidity of the double helix from data on small DNA rings. *J. Biomol. Struct. Dyn.* 2:1005–1012.

19. Vologodskii, A. V., and M. D. Frank-Kamenetskii. 1992. Modeling supercoiled DNA. *Methods Enzymol.* 211:467–480.

20. Hagerman, P. J. 1988. Flexibility of DNA. *Annu. Rev. Biophys. Biophys. Chem.* 17:265–286.

21. Stigter, D. 1977. Interactions of highly charged colloidal cylinders with applications to double-stranded DNA. *Biopolymers.* 16:1435–1448.

22. Rotne, J., and S. Prager. 1969. Variational treatment of hydrodynamic interaction in polymers. *J. Chem. Phys.* 50:4831–4837.

23. Langowski, J., and U. Giesen. 1989. Configurational and dynamic properties of different length superhelical DNAs measured by dynamic light scattering. *Biophys. Chem.* 34:9–18.

24. Hammermann, M., C. Stainmaier, H. Merlitz, U. Kapp, W. Waldeck, G. Chirico, and J. Langowski. 1997. Salt effects on the structure and internal dynamics of superhelical DNAs studied by light scattering and Brownian dynamic. *Biophys. J.* 73:2674–2687.

25. Iniesta, A., and J. G. de la Torre. 1990. A 2nd-order algorithm for the simulation of the Brownian dynamics of macromolecular models. *J. Chem. Phys.* 92:2015–2018.

26. Frank-Kamenetskii, M. D., A. V. Lukashin, and M. D. Vologodskii. 1975. Statistical mechanics and topology of polymer chains. *Nature.* 258:398–402.